Magnetic Resonance Imaging 63 (2019) 49–54

Contents lists available at ScienceDirect

Magnetic Resonance Imaging

journal homepage: www.elsevier.com/locate/mri

Original contribution

Reproducibility of axonal water fraction derived from the spherical mean diffusion weighted signal

Jucai Song[a], Ho Ming Chow[b], Rahul Nikam[c], Vinay Kandula[c], Arabinda K. Choudhary[c], Hua Li[b,*]

[a] Henan Orthopedic Institute, Henan Luoyang Orthopedic Hospital, Zhengzhou, Henan 450000, China
[b] Katzin Diagnostic & Research PET/MR Center, Nemours – Alfred I. duPont Hospital for Children, Wilmington, DE 19803, USA
[c] Department of Radiology, Nemours – Alfred I. duPont Hospital for Children, Wilmington, DE 19803, USA

ARTICLE INFO

Keywords:
Axonal water fraction
Spherical mean signal
Diffusion tensor imaging
Reproducibility

ABSTRACT

Recent years have seen growing interest in measuring axonal water fraction (AWF) using the spherical mean diffusion weighted signal, but information about the reproducibility of this method is needed before applying it in large-scale studies. The current study aims to evaluate the reproducibility of AWF derived from the spherical mean signal method. This retrospective study analyzed the Human Connectome Project (HCP) test-retest diffusion data of ten healthy adults. The diffusion scan was performed two times for each subject. Diffusion tensor imaging-based fractional anisotropy (FA) was calculated with $b = 1000\,s/mm^2$. AWF was calculated with $b = 3000\,s/mm^2$ using the spherical mean signal method. Gradient nonlinearities were corrected in both methods. Reproducibility was assessed using the reproducibility error, which is the percent absolute change relative to the mean. The mean reproducibility error of fractional anisotropy (FA) is 9.7 ± 1.0% in white matter and 18.0 ± 2.0% in gray matter. The mean reproducibility error of AWF is 4.6 ± 0.6% in white matter and 7.0 ± 1.5% in gray matter. Spherical mean signal-based AWF is more reproducible than FA for the HCP high resolution, low signal-to-noise ratio diffusion data.

1. Introduction

Diffusion MRI is an invaluable tool to detect tissue microstructure non-invasively. By varying the gradient direction, one can estimate the main fiber direction [1] or fiber orientation distribution [2]. And by varying the gradient separation or diffusion time, one can measure the fiber size quantitatively [3]. The information provided by varying the gradient strength has also been explored. The conventional diffusion tensor imaging (DTI) [1], which assumes a simple Gaussian model, usually employs a *b*-value of $1000\,s/mm^2$. The derived fractional anisotropy (FA) is used to reflect white matter structural coherence and the derived mean diffusivity (MD) is an important indicator of the level of restricted or hindered diffusion. DTI has been widely used to assess white matter injuries in clinic. The diffusion kurtosis imaging model [4] was developed to describe the non-Gaussian diffusion behavior at *b*-value ~ $2000\,s/mm^2$. The excess kurtosis is estimated to quantify the departure from a Gaussian form. A high *b*-value of $3000\,s/mm^2$ is commonly used in multi-compartment tissue modeling studies [5,6], which provide more specific tissue microstructural information such as axonal water fraction (AWF).

AWF is defined as the ratio of intra-axonal water to the sum of intra- and extra-axonal water. Due to the short T_2 of myelin water, the contribution of myelin water is usually ignored in diffusion models. Since the T_2 difference between intra- and extra-axonal water is not taken into account, AWF is a better terminology than axonal volume fraction or neurite density [7]. Neurite orientation dispersion and density imaging (NODDI) [5] was previously proposed as a clinically feasible approach to measure AWF. However, NODDI is based on several questionable assumptions, such as the simplified Waston fiber orientation distribution and the tortuosity assumption. The assumptions may compromise the specificity of the estimates [8–10]. Recent years have seen growing interest in measuring AWF using the spherical mean diffusion weighted signal [11–16]. The spherical mean diffusion weighted signal is the signal averaged over all gradient directions at the same *b*-value, and it is independent of the underlying fiber orientation distribution when the number of gradient directions is sufficiently large [2,17]. The minimal number of gradient directions for robust measurement of spherical mean signal has been determined recently [18]. When the diffusion weighting *b*-value is sufficiently large, the extra-axonal water contribution is negligible and AWF is simply the product of the spherical mean signal and $2\sqrt{bD/\pi}$, where *D* is the intra-axonal intrinsic diffusivity [19]. Here the measurement of AWF does not

* Corresponding author at: Nemours AI duPont Hospital for Children, 1600 Rockland Road, 1A324, Wilmington, DE 19803, USA.
E-mail address: hua.li@nemours.org (H. Li).

https://doi.org/10.1016/j.mri.2019.08.024
Received 12 April 2019; Received in revised form 23 July 2019; Accepted 15 August 2019

require the tortuosity assumption. Compared with DTI-based FA, spherical mean signal-based AWF is easier to calculate and more appropriate to assess fiber integrity in situations of fiber crossings or fiber dispersions.

The reproducibility of diffusion MRI has been investigated in numerous studies [20–23]. It is imperative to address the test-retest reliability of diffusion metrics before applying them in large-scale studies. Most of the previous reproducibility studies were focused on the conventional DTI model with a single *b*-value of 1000 s/mm^2 and an isotropic image resolution of 2 mm. With the advances of gradient hardware and data acquisition, the Human Connectome Project (HCP) is able to acquire multi-shell diffusion dataset with *b*-value ranging from 1000 s/mm^2 to 3000 s/mm^2 at an isotropic image resolution of 1.25 mm [24,25]. The current study aims to evaluate the test-retest reproducibility of AWF derived from the spherical mean diffusion weighted signal using the HCP test-retest dataset. The reproducibility errors of DTI-based FA and MD were also quantified for comparison. In addition, the effect of gradient nonlinearities on the accuracy of AWF was investigated through computer simulations.

2. Materials and methods

2.1. Data

Test-retest data from ten healthy adults, as part of the WU-Minn Human Connectome Project Retest Data, were downloaded from ConnectomeDB (http://db.humanconnectome.org).The ten subjects were scanned for two times using the same 3 T imaging protocol with a test-retest interval ~ 4 months. Diffusion data were acquired with 3 *b*-values of nominally 1000, 2000 and 3000 s/mm^2. The number of gradient directions was 90 at each shell and the number of $b = 0$ images was 18. For each scan, the diffusion data were acquired twice with opposite phase encoding directions to correct for susceptibility induced image distortions. Other imaging parameters were: TR = 5520 ms, TE = 89.5 ms, gradient duration (δ) = 10.6 ms, gradient separation (Δ) = 43.1 ms, image resolution = 1.25 × 1.25 × 1.25 mm^3, phase partial Fourier = 0.75, and multiband factor = 3. As downloaded, the data were preprocessed with corrections for gradient nonlinearity distortions, susceptibility induced distortions, head motion, and eddy current artifacts [24,25]. During the preprocessing, images acquired with opposite phase encoding directions were combined to obtain the final image. The noise regime of the final image cannot be described by a Rician distribution. Since the noise bias is not expected to affect the test-retest reproducibility results significantly, it was not reduced in the current study. The effect of Rician noise on spherical mean signal was investigated and corrected in previous studies [16,18].

2.2. Data analysis

DTI was analyzed with $b = 1000$ s/mm^2 using FSL [26]. FA and MD were estimated with weighted least squares and correction for gradient nonlinearities. The gradient nonlinearities would alter the strength and direction of diffusion gradients from their nominal values. Thus, the *b*-values and gradient directions were corrected for each voxel as suggested previously [27]. AWF was calculated with $b = 3000$ s/mm^2 using MATLAB (Mathworks, Natick, MA, USA). Without gradient nonlinearities, AWF can be written as [19].

$$\mathrm{AWF} = 2\sqrt{\frac{bD}{\pi}}\cdot\frac{\overline{S}}{S_0} \tag{1}$$

where $\overline{S}$ is the spherical mean diffusion weighted signal and S_0 is the signal for $b = 0$. Eq. (1) was first derived in the fiber-ball imaging work [19]. Details of the derivation can also be found elsewhere [28]. The intra-axonal intrinsic diffusivity D is fixed as 2.25 μm^2/ms based on recent D estimates [14,29]. The gradient nonlinearity corrected AWF is expressed as.

$$\mathrm{AWF} = 2\sqrt{\frac{D}{\pi}}\cdot\frac{\sum_{n=1}^{N}\sqrt{b_n}S_n}{N\cdot S_0} \tag{2}$$

where N is the number of gradient directions, S_n is the measured diffusion weighted signal along the nth gradient direction, and b_n is the corresponding *b*-value after gradient nonlinearity correction. Eq. (2) is an empirical equation. It is a simple expansion of Eq. (1) in the case of varied *b*-values. Eq. (2) was used for AWF measurement on the HCP data.

For each subject, the FA map of scan 1 and the FA map of scan 2 were linearly registered to their halfway space using FSL *flirt* and *midtrans* commands [30]. The MD and AWF maps were then appropriately rotated and registered into the halfway space. The reproducibility error (ε) was then evaluated by calculating the percent absolute change relative to the mean for each diffusion metric (DM) as follows: [22,23].

$$\varepsilon_{\mathrm{DM}} = 100\times\frac{|\mathrm{DM}_{\mathrm{scan1}} - \mathrm{DM}_{\mathrm{scan2}}|}{(\mathrm{DM}_{\mathrm{scan1}} + \mathrm{DM}_{\mathrm{scan2}})/2} \tag{3}$$

where DM refers to any of the three scalar metrics: FA, MD and AWF. Finally, T_1-weighted image was segmented to gray matter (GM), white matter (WM) and cerebrospinal fluid using MRtrix *5ttgen* command [31,32] in order to compute tissue-specific reproducibility. For each subject, the mean $\varepsilon_{\mathrm{DM}}$ over all voxels within a tissue was denoted as $\langle\varepsilon_{\mathrm{DM}}\rangle$. The statistical results of $\langle\varepsilon_{\mathrm{DM}}\rangle$ were given as mean ± standard deviation over all ten subjects.

2.3. Simulations

Computer simulations were performed to investigate the effect of gradient nonlinearities on the accuracy of AWF quantification. The nominal *b*-table and gradient deviation files were from one of the HCP subjects. The gradient deviation in each voxel is a 3 × 3 tensor L. As an example, Fig. 1 (a) shows the first element L_{xx}. The closer the value is to 0, the smaller is the gradient deviation. Simulations were based on a simplified two-compartment analytical model of intra- and extra-axonal spaces [18]. Axons are modeled as randomly placed parallel cylinders and the extra-axonal diffusion is based on the first-order tortuosity approximation [11]. The intra-axonal compartment is a stick compartment. Specifically, $D_{in}^{\perp} = 0$, $D_{ex}^{\perp} = (1 - \mathrm{AWF})\cdot D$, and $D_{in}^{\parallel} = D_{ex}^{\parallel} = D$, where $D_{in}^{\perp}$, $D_{ex}^{\perp}$, $D_{in}^{\parallel}$ and $D_{ex}^{\parallel}$ are intra-axonal radial diffusivity, extra-axonal radial diffusivity, intra-axonal axial diffusivity, and extra-axonal axial diffusivity, respectively. The ground truth AWF is 0.6. Diffusion weighted signals were simulated with the actual *b*-table under gradient deviation. The uncorrected AWF is based on Eq. (1) using the nominal *b*-value of 3000 s/mm^2 and the corrected AWF is based on Eq. (2). To take into account the effect of fiber direction, 10,000 different fiber directions were simulated in each voxel and the mean value was reported as the final result.

3. Results

Fig. 1 (b) and (c) shows the simulated AWF maps before and after correction for gradient nonlinearities. It is evident that gradient nonlinearities would bias the calculation of AWF and that the bias is proportional to the level of gradient deviation. The corrected AWF map is more spatially uniform than the uncorrected one. Fig. 2 shows the histograms of the simulated AWF values before and after correction for gradient nonlinearities. The uncorrected AWF is 0.630 ± 0.015 over all the simulated voxels. The distribution becomes narrower after correction and the corrected AWF is 0.633 ± 0.003. The simulation results demonstrate that Eq. (2) can help reduce the gradient nonlinearity induced bias in AWF measurement on the HCP data.

Fig. 3 shows the test-retest parametric maps and the corresponding

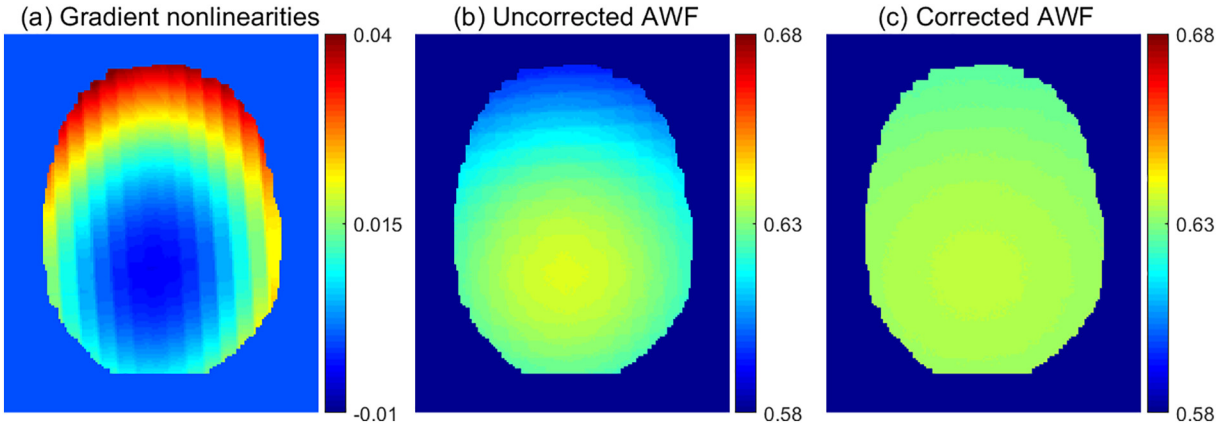

Fig. 1. The first element of the gradient deviation tensor is shown in (a) to illustrate the spatial variations of gradient nonlinearities. The simulated axonal water fraction (AWF) map before correction for gradient nonlinearities is shown in (b), and it was obtained with Eq. (1) using the nominal *b*-value of 3000 s/mm^2. The gradient nonlinearity corrected AWF is shown in (c).

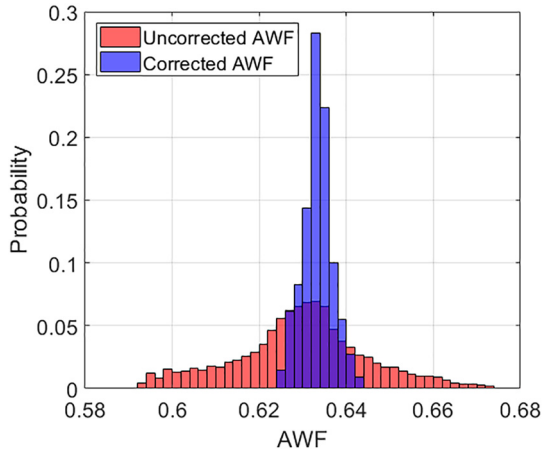

Fig. 2. Histograms of the simulated AWF values before (red) and after correction (blue) for gradient nonlinearities. (For interpretation of the references to colour in this figure legend, the reader is referred to the web version of this article.)

reproducibility errors from a representative subject. Consistent with previous studies [20,21], the reproducibility error of FA is larger in GM than in WM. The reproducibility error maps are more uniform for MD and AWF. Fig. 4 shows the histograms of the reproducibility errors for a specific tissue region (GM or WM) of the same subject shown in Fig. 3. The distributions of ε_{MD} are similar with that of ε_{AWF}. The statistical results of GM and WM mean reproducibility errors over all subjects are listed in Table 1. The WM mean reproducibility error of AWF ($\langle\varepsilon_{AWF}\rangle = 4.6 \pm 0.6\%$) is much smaller than that of FA ($\langle\varepsilon_{FA}\rangle = 9.7 \pm 1.0\%$). The experiment results suggest that AWF is more reproducible than FA for the HCP data.

4. Discussion

The current study assessed the reproducibility of spherical mean signal-based AWF on the HCP data, along with DTI-based FA and MD. DTI was analyzed with $b = 1000$ s/mm^2 and AWF was calculated with $b = 3000$ s/mm^2. Gradient nonlinearities were corrected in both methods. AWF shows smaller mean reproducibility errors than FA in both GM and WM. It suggests that AWF is a more reproducible diffusion metric than FA for the HCP data. The results of this study can be applied to the HCP data and presumably data acquired with a similar protocol, such as the Baby Connectome Project [33] and the Adolescent Brain Cognitive Development study [34].

As reported previously [27], gradient nonlinearities may cause severe spatial variations of the diffusion encoding, especially for high performing gradients. For the 3T HCP diffusion imaging, the actual *b*-values within the brain can deviate up to 15% from the nominal *b*-value [25]. The strong gradient nonlinearities would bias the measured diffusion parameters, which in turn affects the accuracy of the measurements. Thus, gradient nonlinearities should be corrected to obtain the true gradient directions and magnitudes [27]. Besides, the corrected *b*-values along different directions may be slightly different after correction for gradient nonlinearities. Thus, Eq. (2) was proposed to calculate AWF with the *b*-value difference taken into account. While the correction is needed for the HCP scanner, it may not be necessary for standard scanners with much lower gradient nonlinearities [24]. The simulated result of AWF (0.63) is slightly larger than the ground truth AWF (0.6) because the contribution of the extra-axonal water to the total mean signal is not completely negligible at $b = 3000$ s/mm^2 as illustrated in previous simulations [28]. The systematic error is reduced at higher *b*-values [28]. A higher *b*-value was previously recommended to fully suppress the extra-axonal water contribution [35,36]. The differences in AWF when using $b = 3000$ s/mm^2 and $b = 5000$ s/mm^2 (from MGH-USC HCP dataset) have been assessed in a previous work [28]. The spherical mean signal measured at $b = 3000$ s/mm^2 is highly correlated with that measured at $b = 5000$ s/mm^2, which suggests that $b = 3000$ s/mm^2 may be sufficient for spherical mean signal-based AWF measurement in human brain [28].

The reproducibility error of FA in WM observed in this study (~ 10%) is larger than that of other studies (~ 5%) [21,23,37], presumably due to the low SNR of the HCP data. The SNR value is ~ 20 in WM in the final $b = 0$ image. Since the final $b = 0$ image is the combination of two $b = 0$ images acquired with opposite phase encoding directions, it indicates an approximate SNR of 14 in WM in a single $b = 0$ image. The SNR value in a single $b = 0$ image has also been computed in two previous HCP studies [17,25], but with different image resolutions. It was reported that SNR ≈ 45 when image resolution is 2 mm isotropic [25] and SNR ≈ 17.5 when image resolution is 1.5 mm isotropic [17]. Those studies suggest a SNR value of 10–11 for 1.25 mm isotropic image resolution. The estimated SNR value for the HCP data is similar with that of a previous study (SNR = 10) investigating the effect of SNR on the reproducibility of DTI metrics [20]. And the reproducibility results are also similar: FA is less reproducible in GM than in WM and the MD errors are comparable in GM and WM [20]. Besides, MD is more reproducible than FA [20]. It should be noted that the estimation error also depends on the number of measurements and the gradient sampling schemes. Previous studies suggest to use as many unique gradient directions as possible for robust estimations of DTI parameters [20,38].

As shown in Eq. (1), the reproducibility of AWF is equivalent to the

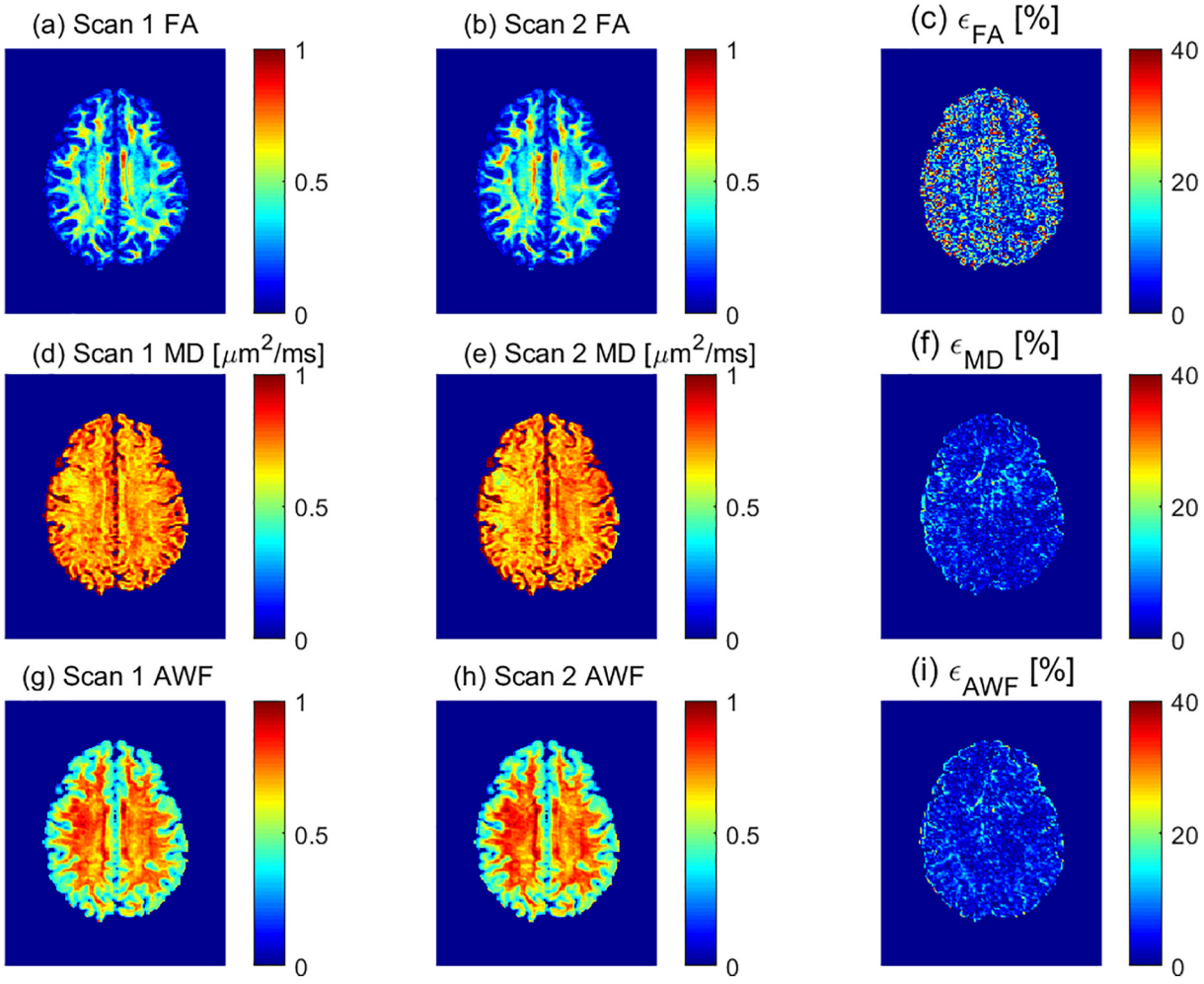

Fig. 3. Fractional anisotropy (FA), mean diffusivity (MD) and AWF maps of a representative Human Connectome Project (HCP) subject scanned for two times. The corresponding reproducibility error maps are shown in the last column.

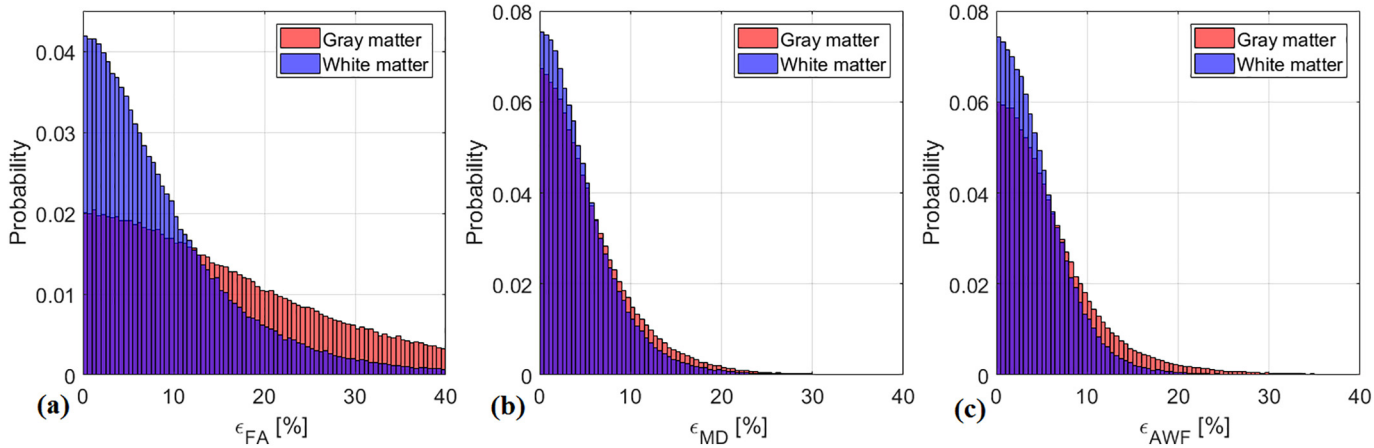

Fig. 4. Histograms of the reproducibility errors for FA (a), MD (b) and AWF (c). Red is for all gray matter voxels and blue for all white matter voxels of the same subject shown in Fig. 3. (For interpretation of the references to colour in this figure legend, the reader is referred to the web version of this article.)

reproducibility of spherical mean diffusion weighted signal after S_0 normalization. The effect of noise on the precision of AWF has been described analytically and validated with simulations [18]. Since the spherical mean signal is the signal averaged over N gradient directions, the noise-induced variance can be estimated as $\frac{1}{SNR \cdot \sqrt{N}}$ [18]. Therefore, a large number of gradient directions can be used to improve the precision of AWF in the situation of low SNR. The voxel-wise reproducibility error of AWF is around 5% in WM, suggesting that AWF is a reliable diffusion metric for the HCP high resolution, low SNR data. As pointed out in the fiber-ball imaging work, Eq. (1) is based on several general assumptions: (1) water can be divided into intra- and extra-axonal pools without exchange between the two pools; (2) the axons can be regarded as sticks with intra-axonal radial diffusivity equal to zero; (3) the *b*-value is sufficiently large so that the extra-axonal water

Table 1
Gray matter and white matter mean reproducibility errors ($\langle\varepsilon\rangle$) over ten subjects. FA = fractional anisotropy; MD = mean diffusivity; AWF = axonal water fraction.

Tissue	$\langle\varepsilon_{FA}\rangle$ [%]	$\langle\varepsilon_{MD}\rangle$ [%]	$\langle\varepsilon_{AWF}\rangle$ [%]
Gray matter	18.0 ± 2.0	6.7 ± 1.4	7.0 ± 1.5
White matter	9.7 ± 1.0	5.2 ± 0.7	4.6 ± 0.6

contribution is negligible; (4) the intrinsic diffusivity D is constant for all the axons within any given voxel. The assumption of a constant intra-axonal intrinsic diffusivity D may not hold true over the whole brain. Several methods [11,12,14,29,39] have been proposed to have an accurate measurement of D, but the results have not been validated yet. The assumption of a constant D has previously been used in the NODDI model [5]. Compared with NODDI or other multi-compartment modeling methods, spherical mean signal-based AWF does not rely on complex fitting procedures. Besides, it only requires a single high b-value to separate intra- and extra-axonal water. The clinical diffusion protocols are usually less than 5 min. Given the limited scanning time in clinic, the single b-value requirement is a significant advantage of the spherical mean signal method for clinical applications. The spherical mean signal method is a fast and simple approach to estimating AWF and shows great potential for clinical applications [16]. It should be noted that the quantification of AWF using Eq. (1) is not accurate in GM [16,35,36]. Recent power law scaling studies [35,36] found that the diffusion behavior in GM is remarkably different from that in WM. However, since the spherical mean signal may still be able to provide some useful information about microstructural changes [40], the reproducibility of spherical mean signal in GM was also investigated in this study. Despite various advanced diffusion models, the diffusion trace is used for almost everything in clinic [8]. The spherical mean signal method is as simple as the diffusion trace. It only requires a higher b-value, but is able to provide more quantitative information. Given this consideration, it is desirable to further explore the clinical potential of AWF derived from the spherical mean diffusion weighted signal.

The current work can be summarized in three points. First, a simple method was proposed to correct for the gradient nonlinearity effect for the spherical mean diffusion weighted signal. This is an interesting topic as demonstrated by the recent abstract investigating gradient nonlinearity correction for spherical mean diffusion imaging [41]. Second, the current study measured the reproducibility errors of DTI metrics on the HCP data. The reproducibility error of FA in WM observed on the HCP data (~ 10%) is larger than that of other studies (~ 5%). This result is important for the studies using the HCP protocol or a similar protocol. Third, the reproducibility error of spherical mean signal-based AWF is around 5%, suggesting that the derived axonal water fraction is a robust diffusion metric for tissue microstructure assessment.

In conclusion, spherical mean signal-based AWF is more reproducible than FA for the HCP data. AWF is a reliable metric for the HCP high resolution, low SNR diffusion data.

Acknowledgement

This work was supported by the National Institutes of Health (grant number R21DC015853). Data were provided by the Human Connectome Project, WU-Minn Consortium (Principal Investigators: David Van Essen and Kamil Ugurbil; 1U54MH091657) funded by the 16 NIH Institutes and Centers that support the NIH Blueprint for Neuroscience Research; and by the McDonnell Center for Systems Neuroscience at Washington University.

References

[1] Basser PJ, Mattiello J, LeBihan D. MR diffusion tensor spectroscopy and imaging. Biophys J 1994;66:259–67. https://doi.org/10.1016/S0006-3495(94)80775-1.
[2] Anderson AW. Measurement of fiber orientation distributions using high angular resolution diffusion imaging. Magn Reson Med 2005;54:1194–206. https://doi.org/10.1002/mrm.20667.
[3] Assaf Y, Blumenfeld-Katzir T, Yovel Y, Basser PJ. AxCaliber: a method for measuring axon diameter distribution from diffusion MRI. Magn Reson Med 2008;59:1347–54. https://doi.org/10.1002/mrm.21577.
[4] Jensen JH, Helpern JA, Ramani A, Lu H, Kaczynski K. Diffusional kurtosis imaging: the quantification of non-Gaussian water diffusion by means of magnetic resonance imaging. Magn Reson Med 2005;53:1432–40. https://doi.org/10.1002/mrm.20508.
[5] Zhang H, Schneider T, Wheeler-Kingshott CA, Alexander DC. NODDI: practical in vivo neurite orientation dispersion and density imaging of the human brain. Neuroimage 2012;61:1000–16. https://doi.org/10.1016/j.neuroimage.2012.03.072.
[6] Raffelt D, Tournier JD, Rose S, Ridgway GR, Henderson R, Crozier S, et al. Apparent fibre density: a novel measure for the analysis of diffusion-weighted magnetic resonance images. Neuroimage 2012;59:3976–94. https://doi.org/10.1016/j.neuroimage.2011.10.045.
[7] Jelescu IO, Budde MD. Design and validation of diffusion MRI models of white matter. Front Phys 2017;5. https://doi.org/10.3389/fphy.2017.00061.
[8] Novikov DS, Kiselev VG, Jespersen SN. On modeling. Magn Reson Med 2018;79:3172–93. https://doi.org/10.1002/mrm.27101.
[9] Lampinen B, Szczepankiewicz F, Mårtensson J, van Westen D, Sundgren PC, Nilsson M. Neurite density imaging versus imaging of microscopic anisotropy in diffusion MRI: a model comparison using spherical tensor encoding. Neuroimage 2017;147:517–31. https://doi.org/10.1016/j.neuroimage.2016.11.053.
[10] Jelescu IO, Veraart J, Fieremans E, Novikov DS. Degeneracy in model parameter estimation for multi-compartmental diffusion in neuronal tissue. NMR Biomed 2016;29:33–47. https://doi.org/10.1002/nbm.3450.
[11] Kaden E, Kelm ND, Carson RP, Does MD, Alexander DC. Multi-compartment microscopic diffusion imaging. Neuroimage 2016;139:346–59. https://doi.org/10.1016/j.neuroimage.2016.06.002.
[12] Novikov DS, Veraart J, Jelescu IO, Fieremans E. Rotationally-invariant mapping of scalar and orientational metrics of neuronal microstructure with diffusion MRI. Neuroimage 2018;174:518–38. https://doi.org/10.1016/j.neuroimage.2018.03.006.
[13] Reisert M, Kellner E, Dhital B, Hennig J, Kiselev VG. Disentangling micro from mesostructure by diffusion MRI: a Bayesian approach. Neuroimage 2017;147:964–75. https://doi.org/10.1016/j.neuroimage.2016.09.058.
[14] McKinnon ET, Helpern JA, Jensen JH. Modeling white matter microstructure with fiber ball imaging. Neuroimage 2018;176:11–21. https://doi.org/10.1016/j.neuroimage.2018.04.025.
[15] Veraart J, Novikov DS, Fieremans E. TE dependent Diffusion Imaging (TEdDI) distinguishes between compartmental T2relaxation times. Neuroimage 2018;182:360–9. https://doi.org/10.1016/j.neuroimage.2017.09.030.
[16] Li H, Nikam R, Kandula V, Chow HM, Choudhary AK. Comparison of NODDI and spherical mean signal for measuring intra-neurite volume fraction. Magn Reson Imaging 2019;57:151–5. https://doi.org/10.1016/j.mri.2018.11.021.
[17] Kaden E, Kruggel F, Alexander DC. Quantitative mapping of the per-axon diffusion coefficients in brain white matter. Magn Reson Med 2016;75:1752–63. https://doi.org/10.1002/mrm.25734.
[18] Li H, Chow HM, Chugani DC, Chugani HT. Minimal number of gradient directions for robust measurement of spherical mean diffusion weighted signal. Magn Reson Imaging 2018;54:148–52. https://doi.org/10.1016/j.mri.2018.08.020.
[19] Jensen JH, Russell Glenn G, Helpern JA. Fiber ball imaging. Neuroimage 2016;124:824–33. https://doi.org/10.1016/j.neuroimage.2015.09.049.
[20] Farrell JAD, Landman BA, Jones CK, Smith SA, Prince JL, Van Zijl PCM, et al. Effects of signal-to-noise ratio on the accuracy and reproducibility of diffusion tensor imaging-derived fractional anisotropy, mean diffusivity, and principal eigenvector measurements at 1.5T. J Magn Reson Imaging 2007;26:756–67. https://doi.org/10.1002/jmri.21053.
[21] Vollmar C, O'Muircheartaigh J, Barker GJ, Symms MR, Thompson P, Kumari V, et al. Identical, but not the same: intra-site and inter-site reproducibility of fractional anisotropy measures on two 3.0T scanners. Neuroimage 2010;51:1384–94. https://doi.org/10.1016/j.neuroimage.2010.03.046.
[22] Jovicich J, Marizzoni M, Bosch B, Bartrés-Faz D, Arnold J, Benninghoff J, et al. Multisite longitudinal reliability of tract-based spatial statistics in diffusion tensor imaging of healthy elderly subjects. Neuroimage 2014;101:390–403. https://doi.org/10.1016/j.neuroimage.2014.06.075.
[23] Albi A, Pasternak O, Minati L, Marizzoni M, Bartrés-Faz D, Bargalló N, et al. Free water elimination improves test–retest reproducibility of diffusion tensor imaging indices in the brain: a longitudinal multisite study of healthy elderly subjects. Hum Brain Mapp 2017;38:12–26. https://doi.org/10.1002/hbm.23350.
[24] Glasser MF, Sotiropoulos SN, Wilson JA, Coalson TS, Fischl B, Andersson JL, et al. The minimal preprocessing pipelines for the Human Connectome Project. Neuroimage 2013;80:105–24. https://doi.org/10.1016/j.neuroimage.2013.04.127.
[25] Sotiropoulos SN, Jbabdi S, Xu J, Andersson JL, Moeller S, Auerbach EJ, et al. Advances in diffusion MRI acquisition and processing in the Human Connectome Project. Neuroimage 2013;80:125–43. https://doi.org/10.1016/j.neuroimage.2013.05.057.
[26] Smith SM, Jenkinson M, Woolrich MW, Beckmann CF, Behrens TEJ, Johansen-Berg

H, et al. Advances in functional and structural MR image analysis and implementation as FSL. Neuroimage 2004;23. https://doi.org/10.1016/j.neuroimage.2004.07.051.
[27] Bammer R, Markl M, Barnett A, Acar B, Alley MT, Pelc NJ, et al. Analysis and generalized correction of the effect of spatial gradient field distortions in diffusion-weighted imaging. Magn Reson Med 2003;50:560–9. https://doi.org/10.1002/mrm.10545.
[28] Li H, Chow HM, Chugani DC, Chugani HT. Linking spherical mean diffusion weighted signal with intra-axonal volume fraction. Magn Reson Imaging 2019;57:75–82. https://doi.org/10.1016/j.mri.2018.11.006.
[29] Dhital B, Reisert M, Kellner E, Kiselev VG. Intra-axonal diffusivity in brain white matter. arXiv Prepr arXiv171204565. 2017.
[30] Jenkinson M, Bannister P, Brady M, Smith S. Improved optimisation for the robust and accurate linear registration and motion correction of brain images. Neuroimage 2002;17:825–41. https://doi.org/10.1016/S1053-8119(02)91132-8.
[31] Tournier JD, Calamante F, Connelly A. MRtrix: diffusion tractography in crossing fiber regions. Int J Imaging Syst Technol 2012;22:53–66. https://doi.org/10.1002/ima.22005.
[32] Zhang Y, Brady M, Smith S. Segmentation of brain MR images through a hidden Markov random field model and the expectation-maximization algorithm. IEEE Trans Med Imaging 2001;20:45–57. https://doi.org/10.1109/42.906424.
[33] Howell BR, Styner MA, Gao W, Yap P-T, Wang L, Baluyot K, et al. The UNC/UMN Baby Connectome Project (BCP): an overview of the study design and protocol development. Neuroimage 2019;185:891–905. https://doi.org/10.1016/j.neuroimage.2018.03.049.
[34] Casey BJ, Cannonier T, Conley MI, Cohen AO, Barch DM, Heitzeg MM, et al. The Adolescent Brain Cognitive Development (ABCD) study: imaging acquisition across 21 sites. Dev Cogn Neurosci 2018;32:43–54. https://doi.org/10.1016/j.dcn.2018.03.001.
[35] McKinnon ET, Jensen JH, Glenn GR, Helpern JA. Dependence on b-value of the direction-averaged diffusion-weighted imaging signal in brain. Magn Reson Imaging 2017;36:121–7. https://doi.org/10.1016/j.mri.2016.10.026.
[36] Veraart J, Fieremans E, Novikov DS. On the scaling behavior of water diffusion in human brain white matter. Neuroimage 2019;185:379–87. https://doi.org/10.1016/j.neuroimage.2018.09.075.
[37] Nencka AS, Meier TB, Wang Y, Muftuler LT, Wu YC, Saykin AJ, et al. Stability of MRI metrics in the advanced research core of the NCAA-DoD concussion assessment, research and education (CARE) consortium. Brain Imaging Behav 2018;12:1121–40. https://doi.org/10.1007/s11682-017-9775-y.
[38] Jones DK. The effect of gradient sampling schemes on measures derived from diffusion tensor MRI: a Monte Carlo study. Magn Reson Med 2004;51:807–15. https://doi.org/10.1002/mrm.20033.
[39] Jensen JH, Helpern JA. Characterizing intra-axonal water diffusion with direction-averaged triple diffusion encoding MRI. NMR Biomed 2018;31. https://doi.org/10.1002/nbm.3930.
[40] Genç E, Fraenz C, Schlüter C, Friedrich P, Hossiep R, Voelkle MC, et al. Diffusion markers of dendritic density and arborization in gray matter predict differences in intelligence. Nat Commun 2018;9. https://doi.org/10.1038/s41467-018-04268-8.
[41] Paquette M, Eichner C, Anwander A. Gradient non-linearity correction for spherical mean diffusion imaging. ISMRM 2019:550.